Available online at www.sciencedirect.com
ScienceDirect
Measurement 40 (2007) 428–436
Measurement
www.elsevier.com/locate/measurement

Measurement of the magnetic field radiating by electrostatic discharges during the verification of the ESD generators

G.P. Fotis *, A.G. Rapanakis, I.F. Gonos, I.A. Stathopulos

School of Electrical and Computer Engineering, Electric Power Department, High Voltage Laboratory, National Technical University of Athens, 9, Iroon Politechniou Str., 15780 Zografou, Athens, Greece

Received 14 February 2006; received in revised form 6 June 2006; accepted 7 June 2006
Available online 8 July 2006

Abstract

This work aims to investigate the transient magnetic field radiating by two commercial generators of electrostatic discharges. Near field measurements have been conducted, a few centimetres away from the discharge point (Pellegrini target). The Pellegrini target is mounted in the centre of a grounded metal plane, inside an anechoic chamber. The measurements are performed in three different directions in relation to the discharge direction. The experimental data show that each ESD generator produces a different transient magnetic field. Furthermore, additional differences in the magnetic field produced by each generator are noted, depending on the direction of the measurement. Finally, comparisons concerning the magnetic field produced by each generator as well as useful conclusions for the decrease of the magnetic field are presented.

Keywords: ESD generators; Magnetic field; Magnetic field sensors; Grounded metal plane

1. Introduction

Electrostatic discharges are quite common in people's every day life and occur rather often, when a transfer of electric charge takes place between two conducting objects with different electrostatic potentials. The probable dangers for humans need further investigation. Therefore, several studies have analyzed the effects of an electrostatic discharge on human health [1,2]. The phenomenon of the electrostatic discharge is more crucial as far as electronic equipment is concerned due to the fact that discharge current could come up to a few Amperes. Despite the fact that such a current lasts only for a few ns, it is quite sufficient to destroy electronic components, especially nowadays that the speed of integrated circuits (CMOS for example) is very high. Greason in [3] made an experimental study of the electrostatic discharge for the charged human body in close approach to various sizes and orientations of an electronic circuit pack near and away from a horizontal ground plane.

* Corresponding author. Tel.: +30 2107723603; fax: +30 2107723504.
E-mail addresses: gfotis@gmail.com (G.P. Fotis), igonos@ieee.org (I.F. Gonos).

0263-2241/$ - see front matter
doi:10.1016/j.measurement.2006.06.011

The IEC 61000-4-2 [4] defines the procedures that must be followed during electrostatic discharges (ESD) tests on electrical or electronic equipment. The specifications in the standard over ESD tests include several parameters, referring to the ESD generator – such as the rise time, the peak or the current at 30 ns and 60 ns. In spite of the fact that several ESD generators fulfill the criteria of the standard, the magnetic field produced by them differs.

Pommerenke's and Frei's investigation [5] on the field produced by various ESD generators, using a grounded metal plane concluded that the field is stronger having the plane vertically positioned rather than having it horizontally positioned. Leuchtmann along with Sroka [6,7] analyzed the electrostatic discharge phenomenon in order to calculate the produced electromagnetic field. A comparison of theoretical data with experimental results showed a totally acceptable agreement for the magnetic field, yet not such a good one for the electric field. Two different field probes were used, giving different results and proving that the measurement of the electromagnetic field is quite a challenging task. It must be noticed that in [7] the authors tried to put the gun in an aluminum foil in order to make the inside of the gun electrically isolated in order to improve the rotational symmetry of the gun. They intended to propose to the IEC Committee in the future to build the ESD generators in a rotational metal case in order to have rotational symmetry of the field.

Benjamin et al. [8] measured the magnetic field produced by electrostatic discharges for various distances from 10 mm to 60 mm showing that the magnetic fields near an ESD can be predicted by a sequence of electric dipoles. Also, the peak of the magnetic field varies inversely to the distance. In another work [9] they measured the optical radiation and the magnetic field generated by ESD together with their current signatures. The measurements showed that during the initial growth the temporal variation of the optical pulse is similar to that of the current.

A recent publication of Pommerenke's team [10] indicates what the next revision of the standard should include. The content of their research shows that the four parameters defined by the standard are deficient; therefore the produced electromagnetic field by the ESD generators should be taken into account in order to define specifications and tolerances.

From the remarks above it is obvious that the study of transient fields is very important and their analysis rather complex at some points. The aim of this work is to contribute to the out coming version of the standard through experiments that have been carried out at the facilities of the High Voltage Laboratory of the National Technical University of Athens in Greece. Throughout these years it was observed that there is a strong probability for the equipment under test (EUT) to pass a test, when conducting measurements using a certain ESD generator and fail when using one other, with in both cases the same charging voltage and to the same discharge current. One main reason for this difference in results on real test objects may be that each ESD generator produces a different electromagnetic field, so the induced voltage differs. The results of this work confirm such differences in measured fields under the same conditions. Furthermore it is noted from the experimental data that each generator may react in a different way on an EUT, depending on its orientation. The asymmetry of the produced electromagnetic fields due to the rotational asymmetry of the high voltage relays that each ESD generator has, is one reason that may affect differently on the same EUT. Such an observation has not been made until present day and should be taken into consideration in the next revision of the standard, in order to define the construction of the future generator, in such a way that radiating electromagnetic fields are the same in all directions. The validity of this approach is proved by the experiments presented in this work.

2. Measurement system

2.1. Experimental set-up

Fig. 1 shows the ESD current experimental set-up. The current and the magnetic field (*H*-field) for charging voltage levels at ± 2 kV were measured simultaneously, by the four-channel Tektronix oscilloscope model TDS 7254B the bandwidth of which ranged from dc to 2.5 GHz. The electrostatic discharges were contact discharges and they were conducted using two Schaffner's ESD generators. The experiment was made only for contact discharges, because there is a reproducibility problem for the air discharges; during the air discharges the produced electric arcs are different and therefore the produced magnetic fields can be compared only if the electric arcs of the air discharges are the same.

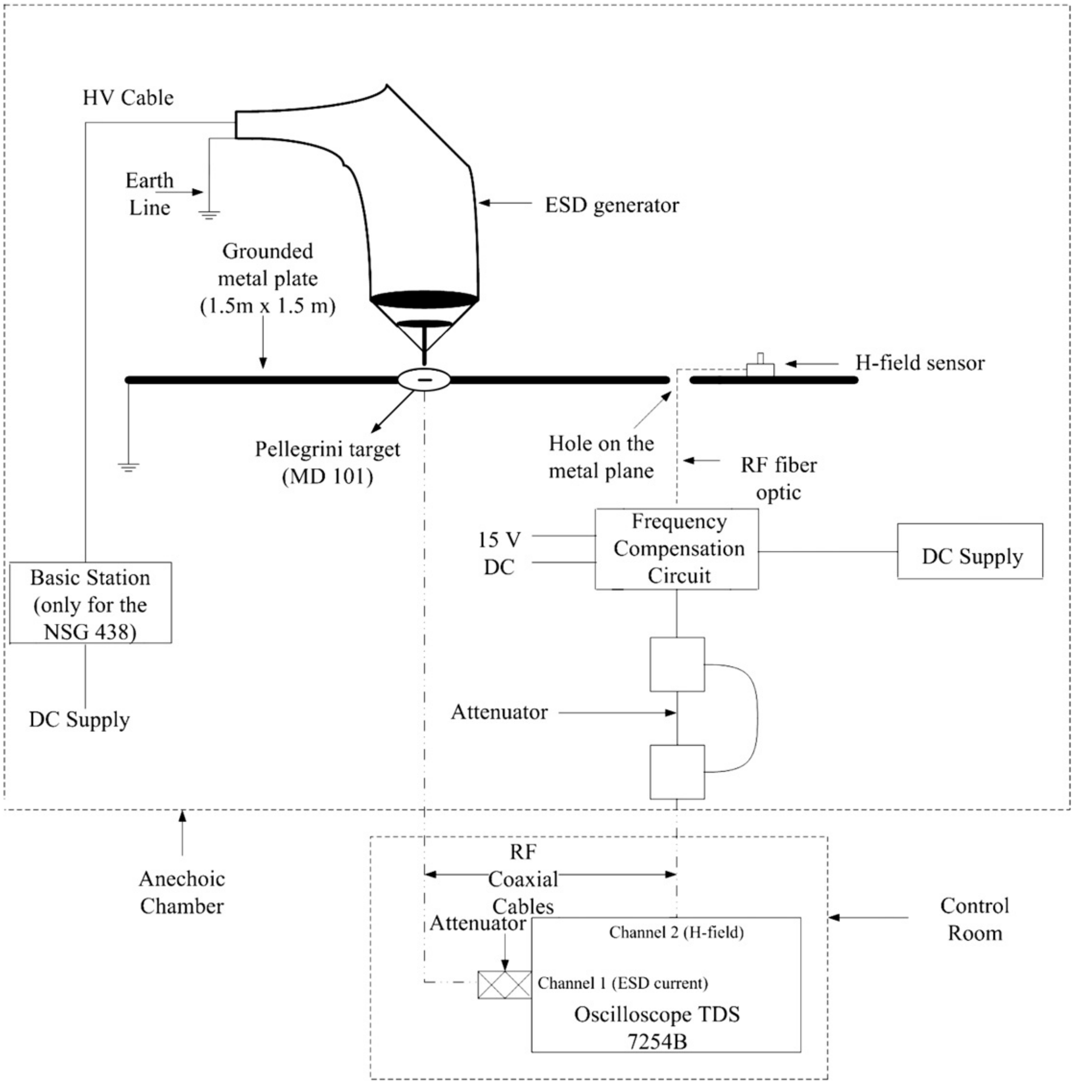

Fig. 1. Experimental set-up.

The ESD generators used were the NSG-433 and the NSG-438. NSG-438 is newer in construction than the NSG-433. It has a touch screen for the selection of the charging voltage and the discharge type (contact or air). They also have differences in their inner circuit, since the charging resistance is 100 MΩ for the NSG-433 and 50 MΩ for the NSG-438. This difference is in accordance to the standard since it defines that the value of the charging resistance must be between 50 and 100 MΩ. It must be mentioned that the NSG 438 had a basic station something that the NSG-433 had not. The basic station of the NSG-438 was on the floor of the anechoic chamber and its horizontal distance from the edge of the grounded metal plane was 40 cm. The positioning of the high voltage cable was kept constant during all the experiment. The high voltage cable positioning of the station was very important and this is a basic difference between the two ESD generators, which affect differently the produced magnetic field.

The temperature and relative humidity were measured and found in the ranges 23 ± 2 °C and $40 \pm 5\%$, respectively. To measure the discharge current a resistive load was used, as defined by the IEC [4]. This resistive load (Pellegrini target MD 101) [11] was designed to measure discharge currents by ESD events on the target area and its bandwidth is ranged from dc to above 1 GHz. The Pellegrini target was placed on a horizontal metal plane with dimensions $1.5 \times 1.5\ \mathrm{m}^2$, which was placed 70 cm above the ground.

The sensor that was used for the experiment was an H-field sensor of Pommerenke [12]. The sensor was placed at various distances (20, 35, 50 and 65 cm) on the metal plane and in three perpendicular directions (direction A, direction C and direction D) on the horizontal plane as it can be seen in Figs. 2 and 3. Measurements in direction B were not conducted due to the interference that the ground strap of the ESD generator was causing. It is known that the position of the ground strap affects the falling edge of the current waveform. In order to minimize the uncertainty associated with this fact into the measurement of the magnetic field, the ground strap was at a distance of 1 m from the target as defined in the standard and its loop was as large as possible. At each point, as it can be seen by Fig. 2(a), six measurements were conducted measuring each time the discharge current and the magnetic field. This was done in order to calculate the average and the standard deviation of the magnetic field at each point. Fig. 2(b) shows the position of the H-field sensor in relation to the Pellegrini target on the grounded metal plane.

2.2. Reconstruction of the current

In the oscilloscope the measured magnitude is the voltage. Therefore the reconstruction of the measured voltage into current is necessary. The most accurate way to reconstruct the current is described by Sroka [13] using the measurement chain as given in Fig. 3. The low frequency transfer impedance of a target/attenuator/cable chain is defined as the ratio between the current injected at the front face of the target and the voltage across a precision 50 Ω load at the output end of the cable. P_{cable} and P_{target} are chain matrixes. By cascade connection of two two-ports (in our case target and cable with attenuator) the calculation of the equivalent chain matrix is made possible.

For the chain matrix of the target the following formula is valid:

$$P_{\mathrm{target}} = \begin{bmatrix} A' & B' \\ C' & D' \end{bmatrix} = \begin{bmatrix} 1 & R_2 \\ \frac{1}{R_1} & 1 + \frac{R_2}{R_1} \end{bmatrix}, \tag{1}$$

where R_1 is target resistance to ground and R_2 is target resistance between input and output.

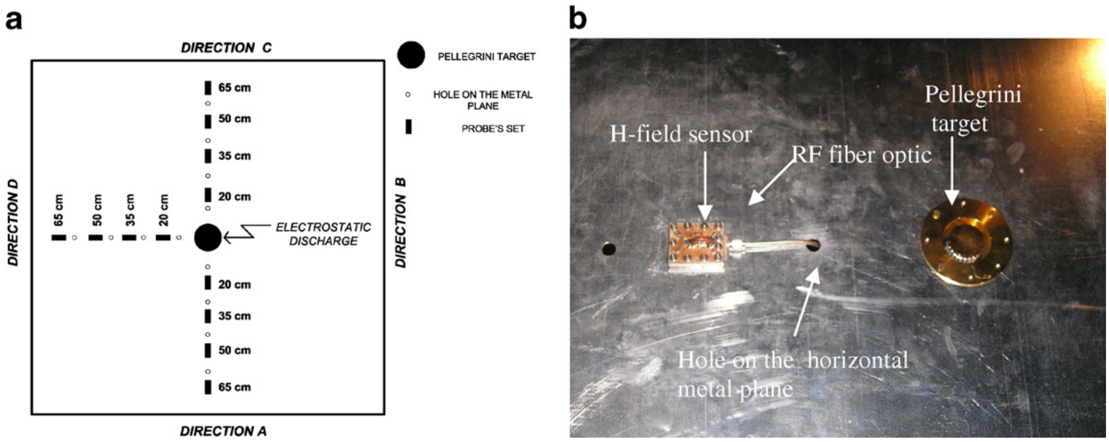

Fig. 2. (a) The measurement points where the H-field sensor was placed. (b) Position of the H-field sensor on the grounded metal plane.

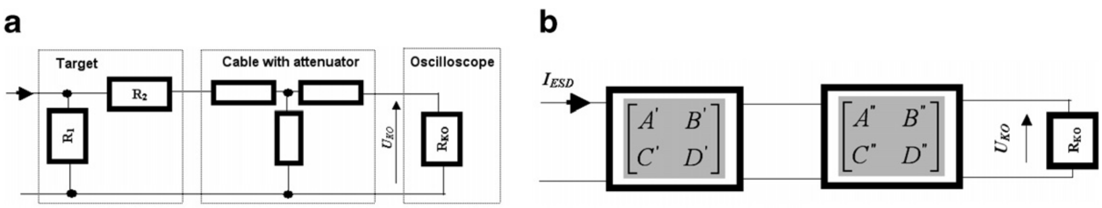

Fig. 3. The equivalent circuit of the ESD generator at DC analysis.

For the chain matrix of the cable with the attenuator the following formula is valid:

$$P_{\text{cable}} = \begin{bmatrix} A'' & B'' \\ C'' & D'' \end{bmatrix} = \begin{bmatrix} \frac{1+d^2}{2\cdot d} & \frac{25}{d}\cdot(1-d^2) \\ \frac{1-d^2}{100\cdot d} & \frac{1+d^2}{2\cdot d} \end{bmatrix}, \tag{2}$$

where d is rated attenuation of the attenuator in linear scale:

$$d = \frac{1}{10^{\frac{A}{20}}} \tag{3}$$

A is the attenuation in dB. In our case since $A = 20$ dB, d equals to 0.1.

By conducting measurements easily can be found that $R_1 = 2.018\ \Omega$ and $R_2 = 48.964\ \Omega$. Multiplying (1) with (2) the chain matrix of cascade junction of two two-ports is easily derived.

$$\begin{bmatrix} A & B \\ C & D \end{bmatrix} = P_{\text{target}} \cdot P_{\text{cable}} \approx \begin{bmatrix} 9.8974 & 494.7682 \\ 5.0034 & 250.2174 \end{bmatrix}. \tag{4}$$

The transfer admittance as the recalculation coefficient between displayed voltage on the oscilloscope and discharge current is given by (5). Also, assuming that R_{KO} equals to 50 Ω, the discharge current is derived as a function of the output voltage.

$$Y_{\text{TRAN}} = \frac{i_{\text{ESD}}(t)}{u_{\text{KO}}(t)} = C + \frac{D}{R_{\text{KO}}} \Rightarrow I_{\text{ESD}} = 10.0077 \cdot V_{\text{out}}. \tag{5}$$

Taking all the above into consideration, the voltage reading of 1 V at the oscilloscope corresponds to the discharge current of ≈10 A.

2.3. H-field sensors

The H-field sensor is ground based field sensor with active integration using a GaAs impedance converter for the sensor. It is rectangular in shape and it is about 4 cm × 3 cm × 1 cm. The H-field sensor covers an area of 0.0012 m^2 on the metal plane, when the metal plane has a total surface of 2.25 m^2. The dynamic range of the H-field sensor is 0.1 A/m to 200 A/m. When measured in an open strip line the sensor exhibits a ±1.5 dB frequency response from 2.5 MHz to 2 GHz. The sensitivity of the sensor is 124.14 μV(V/m) and it can be determined by calibration, using frequency response set-up. The set-up for the calibration of the sensor requires to a strip line and a network analyzer. A detailed analysis of the sensor and its calibration can be found in [12]. The construction of this sensor is made by Pommerenke and is not commercially available.

3. Experimental results

The magnetic field strength was calculated using the experimental set-up described in Section 2.1. Next, representative waveforms of the magnetic field strength in relation to the discharge current are depicted for two different charging polarities (Figs. 4 and 5). It is obvious that the magnetic field is proportional to the discharge current according to Ampere's law that relates the magnetic field strength with the current using the following equation: $H = \frac{I}{2\pi R}$. It can be also observed that the magnetic

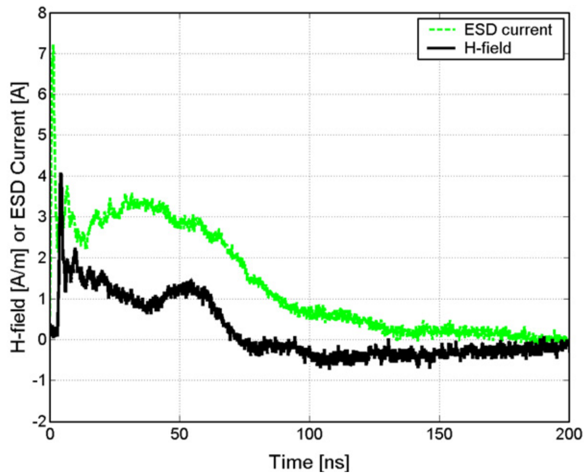

Fig. 4. ESD current and H-field for the NSG-438 ESD generator at 20 cm from the discharge point, in direction A (charging voltage = +2 kV).

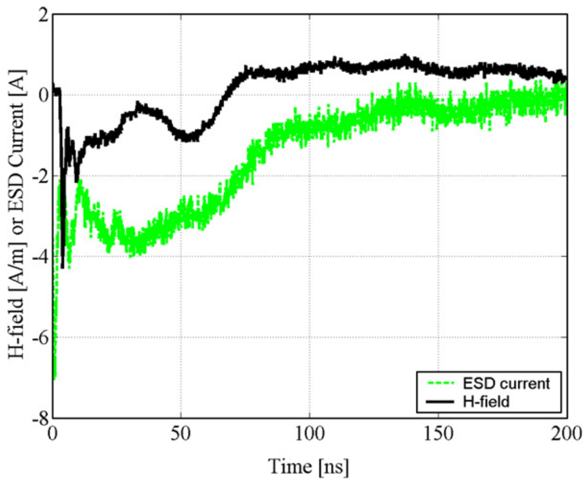

Fig. 5. ESD current and H-field for the NSG-438 ESD generator at 20 cm from the discharge point, in direction A (charging voltage = −2 kV).

field starts with a flat line for the first few ns. The electromagnetic wave covers the distance of 20 cm in about 0.7 ns. The other 2 ns are due to the delay of the field sensor. Superposition of wave delay and probe results in a total delay of about 3 ns.

The peaks of the magnetic field strength (H_{max}) for both NSG-433 and NSG-438 and for all three directions are presented in Figs. 6–8. The amplitude of the peak H-field decreases as the distance between the discharge point and the magnetic field sensor increases. This is in accordance to the remarks of [5], where comparisons of the magnetic field for the metal plane in horizontal position were made. It should be also underlined that the two ESD generators produce different magnetic fields due to differences in their construction and probably due to the different relay they are equipped with. It can be seen in all three figures that the magnetic field strength decreases as the distance increases, according to the $1/R$ factor (R is the distance from the discharge point). In direction C and D the magnetic field strength of the NSG-438 is higher than this of the NSG-433. Also, the magnetic field strength for positive charges is higher than this when the charge is negative. This conclusion is not valid for direction A, where NSG-433 produces in general higher magnetic field than the NSG-438 and also negative charges produce higher field than this that positive charges produce. It must be mentioned that for the negative discharges we have higher discharge current and consequently higher magnetic field strength, but the discharge current is within the limits defined by the standard [4] for the calibration procedure.

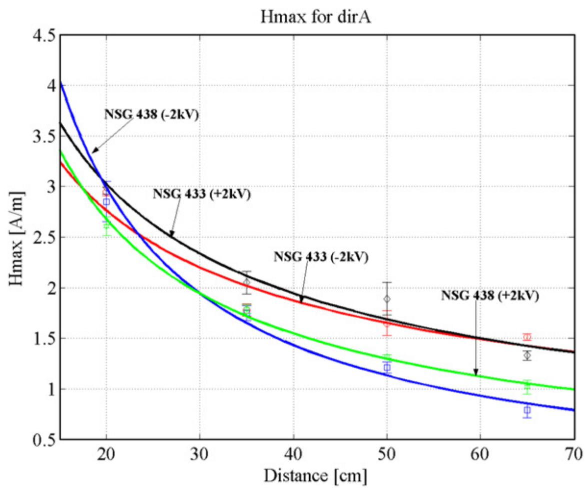

Fig. 6. Peak of H-field for various distances from the discharge point in direction A, using the NSG-433 and NSG-438 ESD generators.

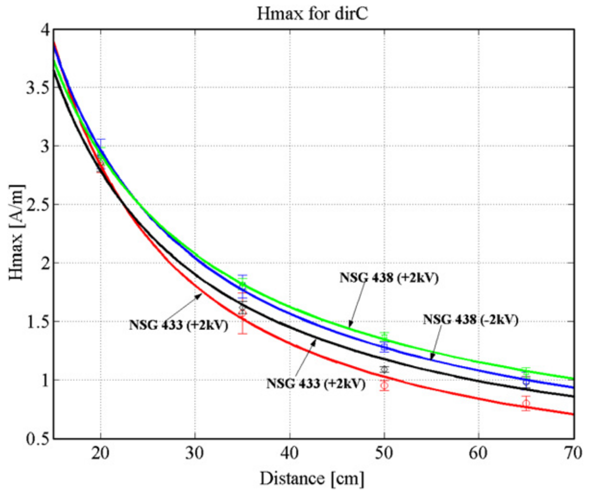

Fig. 7. Peak of H-field for various distances from the discharge point in direction C, using the NSG-433 and NSG-438 ESD generators.

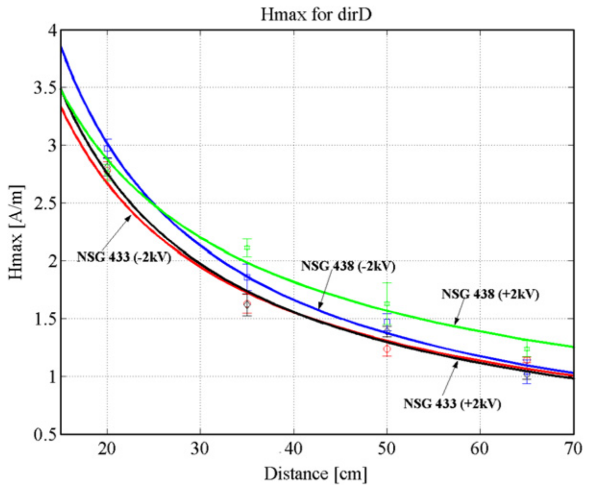

Fig. 8. Peak of H-field for various distances from the discharge point in direction D, using the NSG-433 and NSG-438 ESD generators.

During the measurements, different magnetic field was noted at perpendicular directions, for the same discharge voltage, the same metal plane, the same distance between the sensor and the discharge point and of course for the same ESD generator. The following Figs. 9–12 show the comparison between the peaks of the absolute value of the magnetic field for all three directions. It is made clear that as far as the NSG-433 ESD generator is concerned, the field generated in direction A is stronger

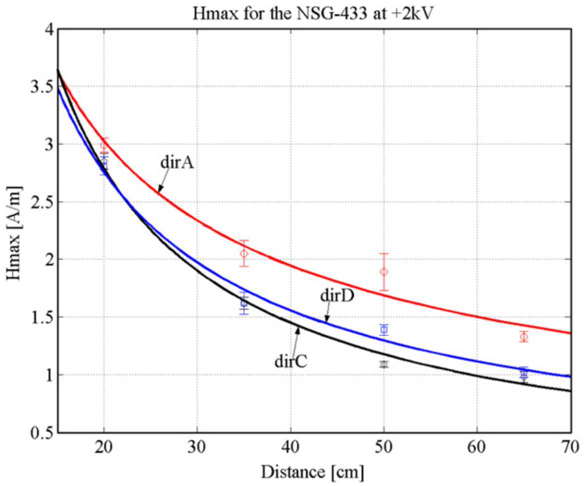

Fig. 9. Peak of magnetic field strength for the NSG-433 ESD generator for three perpendicular directions on the horizontal plane (charging voltage = +2 kV).

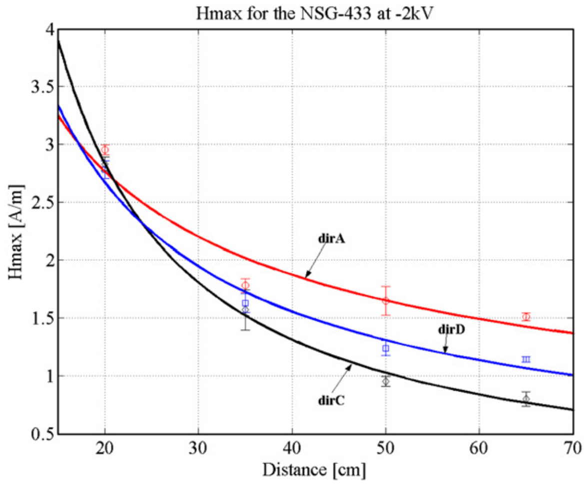

Fig. 11. Peak of magnetic field strength for the NSG-433 ESD generator for three perpendicular directions on the horizontal plane (charging voltage = −2 kV).

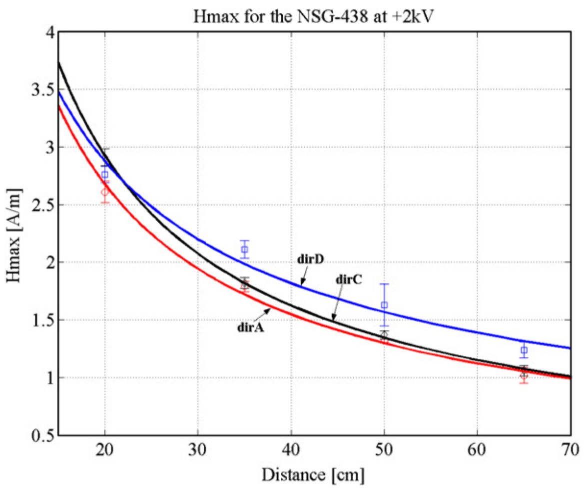

Fig. 10. Peak of magnetic field strength for the NSG-438 ESD generator for three perpendicular directions on the horizontal plane (charging voltage = +2 kV).

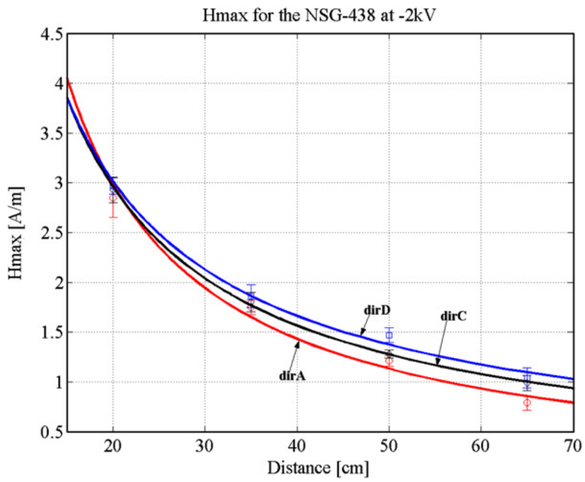

Fig. 12. Peak of magnetic field strength for the NSG-438 ESD generator for three perpendicular directions on the horizontal plane (charging voltage = −2 kV).

than the one generated in direction *D*. Moreover the field generated in direction *D* is stronger than the one generated in direction *C*. So the directions in which the *H*-field peak is higher can be sorted as follows: direction *A* > direction *D* > direction *C*. In the case of the NSG-438 ESD generator the field generated in direction *D* is stronger than the one generated in direction *C*. Moreover the field generated in direction *A* is stronger than the one generated in direction *C*. So the directions in which the peak of the *H*-field is higher can be sorted as follows: direction *D* > direction *C* > direction *A*. These differences could be explained assuming that the circuit produces different magnetic field around it. Great attention should be paid to this fact because the orientation of the ESD generator could result in a different way on the EUT. For example if a test is carried out using the NSG-433 ESD generator and having the EUT placed in direction *C* the result may be positive. On the other hand the same EUT may fail the exact same test if placed in direction *A* because in this direction the peak field is higher. It must be mentioned that different test results on the EUT may be obtained by different ESD generators. If the ESD generator is changed and even if the ESD generator's direction is the same the produced magnetic field is different and therefore the test result on the EUT may be different.

4. Conclusions

An experimental approach has been carried out in order to investigate the transient magnetic fields associated with the electrostatic discharges. The transient magnetic fields produced by two different ESD generators and for charging voltages at ± 2 kV were measured, when the Pellegrini target was mounted on a grounded metal plane. The comparisons showed that each generator produces a different magnetic field and due to this fact different results may be obtained when an EUT is tested. Therefore, there is a need for the next revision of the IEC 61000-4-2 to take into consideration this remark, in order to define and unify the limits of the produced transient fields. Also, it was found that each ESD generator produces different magnetic fields depending on the direction that the measurement is carried out. This means that there are differences in the produced magnetic field not only from generator to generator but for the same generator as well. This means that depending on the orientation of the ESD generator the induced voltages are different and therefore an EUT may pass the test with one orientation of the ESD generator and fail with another. It was also confirmed that the magnetic field is decreased as the distance from the discharge point increases inversely to the distance.

There is rotational asymmetry of the field distribution around the ESD generators, which may affect differently an EUT. Two possible reasons for this phenomenon are: (a) inside of the ESD generator the high voltage relays have not rotational symmetry, (b) the positioning of the return path and additionally the high voltage cable of the NSG-438 have influence on it. It must be also mentioned that in the calibration set-up the positioning of these cables can be defined and the field measurements can be reproducible, but testing an EUT the positioning of these cables is not defined and the reproducibility of the field distribution is much weaker. The IEC Committee should take under consideration in the future revision of the standard that the ESD generators should be marked on the direction that the field is the highest. Also, during the verification the ESD generators should be tested on the produced electromagnetic field around 360°.

As summary, some possible suggestions for the next revision of the IEC 61000-4-2 are: (a) The revised standard should define the construction of the ESD generators that will ensure the uniformity of the magnetic field around the ESD generator. This would minimize the uncertainty of the ESD tests. If this is not possible then perhaps the ESD generators should be marked on the direction that the field is highest on the direction of which the ESD tests would take compulsory take place. This would increase the reliability of the ESD tests. (b) During the verification, the produced electromagnetic field of the ESD generators should be tested around 360°. (c) The next revision of the standard should include typical waveforms of the magnetic field that is produced by electrostatic discharges. (d) In the revised standard the magnitudes of the magnetic field (such as $H_{\max}$, the rise time of the peak magnetic field strength and perhaps values for the derivatives of the produced magnetic field). Should the above remarks be taken into consideration in the next revision of the standard and particularly in the specifications for the design of the ESD generators, the test result uncertainty will be reduced.

Acknowledgements

G.P. Fotis, who is a Ph.D. student thanks the State Scholarships Foundation of Greece for his financial support.

The authors would also like to thank Professor David Pommerenke of the Missouri-Rolla University in the USA and Dr. Jan Sroka of Schaffner for their very useful comments and technical support of the work presented here.

References

[1] E. Okoniewska, M.A. Stuchly, M. Okoniewski, Interactions on electrostatic discharge with the human body, IEEE Trans. Microwave Theory Tech. 52 (2004) 2030–2039.

[2] G. Decat, M. Wevers, P. Kessels, G. Meynen, K. Scheepers, K. Duyssens, L. Deckx, P. Van Tichelen, Z. Grabarczyk, G.P. Fotis, Is electrostatic discharge produced under office working conditions in such a way that it can trigger lipoatrophia semicircularis? In: Proceedings of the International Workshop on Electromagnetic Fields in the Workplace, Warszawa, Poland, September 5–7 (2005) 17–22.

[3] W.D. Greason, Electrostatic discharge characteristics for the human body and circuit packs, J. Electrostat. 59 (2003) 285–300.

[4] IEC 61000-4-2: Electromagnetic Compatibility (EMC), Part 4: Testing and measurement techniques, Section 2: Electrostatic discharge immunity test – Basic EMC Publication.

[5] S. Frei, D. Pommerenke, Fields on the horizontal coupling plane excited by direct ESD and discharges to the vertical coupling plane, J. Electrostat. 44 (1998) 177–190.
[6] P. Leuchtmann, J. Sroka, Transient field simulation of electrostatic discharge (ESD) in the calibration setup (acc. IEC 61000-4-2). In: Proc. of IEEE Int. Symp. on EMC (2000) 443–448.
[7] P. Leuchtmann, J. Sroka, Enhanced field simulations and measurements of the ESD calibration setup. In: Proc. of IEEE Int. Symp. on EMC (2001) 1273–1278.
[8] J. Bendjamin, R. Thottappillil, V. Scuka, Time varying magnetic fields generated by human metal (ESD) electrostatic discharges, J. Electrostat. 46 (1999) 259–269.
[9] J. Bendjamin, C. Gomes, V. Cooray, Remote sensing of ESD through optical and magnetic radiation fields, IEEE Trans. Dielectrics Electr. Insulation 6 (1999) 896–899.
[10] R. Chundru, D. Pommerenke, K. Wang, T.M. Doren, F. Centola, J. Huang, Characterization of human metal ESD reference discharge event and correlation of generator parameters to failure levels. Part 1: Reference event, IEEE Trans. EMC 46 (2004) 498–504.
[11] J. Sroka, Target influence on the calibration uncertainty of ESD simulators. In: Proc. of 14th Int. Symp. and Exhibition on EMC, Zurich (2001) 189–192.
[12] K. Wang, D. Pommerenke, R. Chundru, T.V. Doren, J.L. Drewniak, A. Shashindranath, Numerical modeling of electrostatic discharge generators, IEEE Trans. EMC 45 (2003) 258–271.
[13] J. Sroka, Recalculation of the discharge current from the oscilloscope reading applied by the Schaffner Calibration Laboratory in Luterbach Schaffner's Technical Document.